International Journal of Mining Science and Technology 32 (2022) 1115–1124

Contents lists available at ScienceDirect

International Journal of Mining Science and Technology

journal homepage: www.elsevier.com/locate/ijmst

Composite rock-breaking of high-pressure CO_2 jet & polycrystalline-diamond-compact (PDC) cutter using a coupled SPH/FEM model

Can Cai [a,b,c,d,*], Pei Zhang [a,c], Daping Xu [e], Xianpeng Yang [a,c], Yingfang Zhou [d]

[a] School of Mechanical Engineering, Southwest Petroleum University, Chengdu 610500, China
[b] Key Laboratory of Groundwater Resources and Environment, Jilin University, Ministry of Education, Changchun 130021, China
[c] Laboratory of High-pressure Jet Theory and Application Technology, Southwest Petroleum University, Chengdu 610599, China
[d] School of Engineering, University of Aberdeen, Aberdeen AB24 3FX, United Kingdom
[e] School of Intelligent Manufacturing, Panzhihua University, Panzhihua 617000, China

ARTICLE INFO

Article history:
Received 19 March 2022
Received in revised form 13 May 2022
Accepted 25 August 2022
Available online 3 September 2022

Keywords:
CO_2 drilling
High-pressure CO_2 jet & PDC cutter
Composite rock-breaking
Experimental study
SPH/FEM method

ABSTRACT

CO_2 drilling is a promising underbalance drilling technology with great advantages, such as lower cutting force, intense cooling and excellent lubrication. However, in the underbalance drilling, the mechanism of the coupling CO_2 jet and polycrystalline-diamond-compact (PDC) cutter are still unclear. Whereby, we established a coupled smoothed particle hydrodynamics/finite element method (SPH/FEM) model to simulate the composite rock-breaking of high-pressure CO_2 jet & PDC cutter. Combined with the experimental research results, the mechanism of composite rock-breaking is studied from the perspectives of rock stress field, cutting force and jet field. The results show that the composite rock-breaking can effectively relieve the influence of vibration and shock on PDC cutter. Meanwhile, the high-pressure CO_2 jet has a positive effect on carrying rock debris, which can effectively reduce the temperature rising and the thermal wear of the PDC cutter. In addition, the effects of CO_2 jet parameters on composite rock-breaking were studied, such as jet impact velocity, nozzle diameter, jet injection angle and impact distance. The studies show that when the impact velocity of the CO_2 jet is greater than 250 m/s, the CO_2 jet could quickly break the rock. It is found that the optimal range of nozzle diameter is 1.5–2.5 mm, the best injection angle of CO_2 jet is 60°, the optimal impact distance is 10 times the nozzle diameter. The above studies could provide theoretical supports and technical guidance for composite rock-breaking, which is useful for the CO_2 underbalance drilling and drill bit design.

1. Introduction

Petroleum and natural gas resources are the main energy sources in today's human society, it affects people's livelihood and national defense security. With the continuous improvement of petroleum and natural gas exploration and development, the number of deep and ultra-deep wells has gradually increased, the geological conditions have become more and more complex [1]. Conventional drilling and completion methods are more and more restricted, making it difficult to meet the requirements of economic development [2]. Therefore, efficient and low-cost drilling technology has become a research hotspot in the petroleum industry.

The drilling medium plays a dominant role in the drilling process, which is essential for efficient drilling. Compared with water, carbon dioxide (CO_2) fluid is used in gas drilling due to its low viscosity, high diffusion coefficient and high solubility. At the same time, the shortage of water resources, the urgent demand for shale gas exploration and the greenhouse effect caused by a large amount of CO_2 produced by the coal chemical industry have become prominent [3]. CO_2 has wide application prospects in the industrial field due to its advantages of low manufacturing cost, stable chemical properties and high safety [4]. In the resource development field, CO_2 has become a new rock breaking medium and its potential application value is being further developed. For example, CO_2 is used as the fracturing fluid, using supercritical carbon dioxide (SC-CO_2) hydraulic jet fracturing technology to improve the oil recovery rate and storge of CO_2 [5–9]. Another example is that CO_2 fluid is used as drilling fluid in gas drilling. With the development of underbalance gas drilling technology, low-temperature jet rock breaking of gas drilling fluid is expected to open up a new way of jet rock breaking [10]. In 2000, Kolle et al, took the lead in the experiment of SC-CO_2 jet assisted coiled tubing

* Corresponding author.
E-mail address: cainia10@163.com (C. Cai).

https://doi.org/10.1016/j.ijmst.2022.08.009
2095-2686/

drilling. The results show that SC-CO_2 jet can effectively reduce the threshold pressure of rock breaking [11]. SC-CO_2 jet-assisted radial drilling is regarded as a potential alternative drilling method, because SC-CO_2 jet has higher efficiency in rock-breaking than water jet [12]. And SC-CO_2 (304.1 K, 7.38 MPa) is much easier to be generated than other common materials. It has a density of approximate 0.75 g/cm^3 under the bottom-hole condition of 353 K and 20 MPa, not much less than that of the water (1 g/cm^3). Thus, it can provide sufficient torque for the down-hole motor while drilling. The density of CO_2 fluid decreases continuously as it rises to the ground and a certain section of CO_2 in the annulus is gaseous. As both underbalance or overbalance drilling conditions can be controlled by adjusting the opening of the throttle valves at the wellhead, it is expected to improve the drilling rate markedly [13]. At the same time, when CO_2 jet impacts the rock surface, it is easier for CO_2 than for water to expand into the micropores and microcracks, leading to large damage distribution for the rock. After volume expansion and pressure relief, a relatively large tensile stress can be formed around the rock crushing pit, which reduces the threshold pressure of rock breaking and improves the rock breaking efficiency [14]. The strong permeability and low temperature cooling effect of gas jet can enhance the rock breaking efficiency [15]. With the development of jet drilling technology, a large number of experts have carried out a lot of research on water jet rock breaking [16], SC-CO_2 jet rock breaking [17] and single PDC cutter cutting [18,19]. By using arbitrary lagrange euler-finite element method (ALE-FEM) [20], SPH-FEM [21,22] and other coupled method, the simulation study of the jet rock breaking mechanism is carried out. However, there are relatively fewer researches on the composite rock-breaking of high-pressure CO_2 jet & PDC cutter, which would limit the development and application of CO_2 drilling in future exploitation.

Therefore, we propose the composite rock-breaking of a high-pressure CO_2 Jet & PDC cutter [23]. Combined with the completed research [24], it can be found that the composite rock-breaking of high-pressure CO_2 jet & PDC cutter can effectively inhibit the heat generation of PDC cutter, reduce the thermal wear rate of the PDC cutter, and also improve the capacity of drill bit cleaning and debris carrying. Through the preliminary experimental research, the experiment of composite rock-breaking was designed, and the principle of the experiment is shown in Fig. 1. We also established the model of the composite rock-breaking of high-pressure CO_2 jet & PDC cutter by using a novel SPH/FEM method. Combined with the experimental and numerical studies, the mechanism of composite rock-breaking is explored from the perspectives of rock stress field, cutting force and jet field. The influence of CO_2 jet parameters on composite rock-breaking is further explored, such as jet impact velocity, nozzle diameter, jet injection angle and impact distance. The optimal nozzle arrangement and working parameters are obtained through the research to improve the rock-breaking efficiency of composite rock-breaking. This study could provide theoretical support and technical guidance for composite rock-breaking of high-pressure CO_2 jet & PDC cutter, which is useful for the CO_2 underbalance drilling and drill bit design.

2. Coupled SPH/FEM method and numerical model

2.1. Coupled SPH/FEM method

In the rock breaking by using CO_2 jet impingement, both fluid flow injection and high-amplitude shock waves are involved. The large deformation and high strain rate of CO_2 exist in the rock breaking process by CO_2 jet impacts. The calculation would easily terminate due to the mesh distortion while adopting the conventional Lagrangian finite element method (FEM). Smoothed particle hydrodynamics (SPH) is a mesh-free particle method in the Lagrangian frame, the mesh distortion can be well avoided due to no structural mesh among these particles [25]. Therefore, it is a powerful method to solve the problems of multi-physics flow and large deformation. In this paper, the coupled SPH/FEM method was adopted to simulate the rock fragmentation process induced by the CO_2 jet impacts [26]. The basic idea is to combine the characteristics of the SPH method suitable for large deformation and the advantages of the high efficiency of FEM to improve the calculation accuracy and efficiency of the numerical algorithm [27]. The coupled SPH/FEM method consists of two models, the rock model is established by FEM and the CO_2 jet model is established by SPH.

2.1.1. Theory of SPH and model of CO_2 jet

As the CO_2 jet shows the feature of drastic volume expansion in the free field, the SPH method is well suited for its numerical modeling [21,22]. The SPH method, which is based on the interpolation

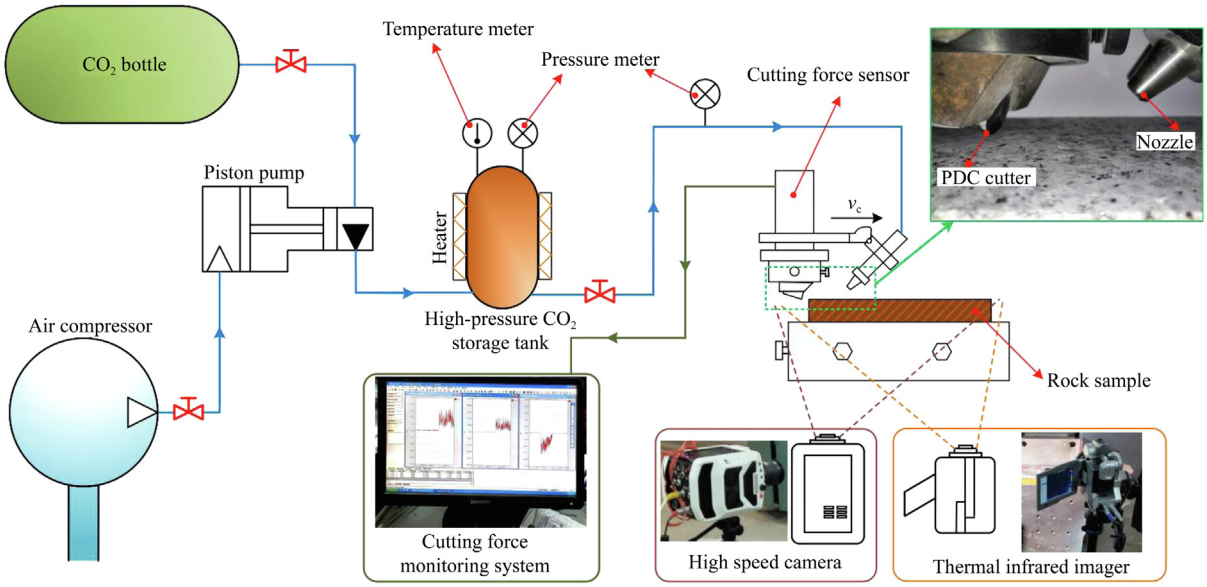

Fig. 1. Schematic of the composite rock-breaking experiment.

theory, allows any function to be expressed at a set of disordered points which represents particle positions via smooth kernel function.

For the function value of a particle in any domain Ω, it can be expressed by smooth kernel function $W(x–x',h)$ as follows:

$$f(x)=\int_{\Omega} f(x')W(x-x',h)\mathrm{d}x' \tag{1}$$

where $f(x)$ is a three-dimensional coordinate function of x; $(x–x')$ is the distance between two particles; and h the smooth length that defines the supporting domain of the particle.

Using the divergence theory to transform the above equation into the spatial derivative of the kernel function:

$$\nabla f(x_i)=\int_{\Omega}[\nabla f(x')]W(x-x',h)\mathrm{d}x' \tag{2}$$

The discretized differential form at point i can be respectively expressed as follow:

$$\nabla f(x_i)=\sum_{j=1}^{n}\frac{m_j}{\rho_j}f(x_j)\cdot\nabla_i W_{ij} \tag{3}$$

where m_j is the mass of particle j; ρ_j the density of particle j; n the total number of particles; and W_{ij} the smooth kernel function, $W_{ij}=W(x_i–x_j,h)$.

The equations of conservation governing the evolution of mechanical variables can be expressed as follows (Eqs. (4)–(6)):

Conservation of mass:

$$\frac{\mathrm{d}\rho_i}{\mathrm{d}t}=\sum_{j=1}^{n}m_j v_{ij}^{\beta}\frac{\partial W_{ij}}{\partial x_i^{\beta}} \tag{4}$$

where v_{ij}^{β} is the relative velocity between two particles in β direction; and x_i^{β} the coordinate of particle i in β direction.

The momentum conservation equation in Lagrange form is:

$$\frac{\mathrm{d}U^{\alpha}}{\mathrm{d}t}=-\frac{1}{\rho}\frac{\partial P}{\partial x^{\alpha}}+\frac{1}{\rho}\frac{\partial \tau^{\alpha\beta}}{\partial x^{\beta}}+F^{\alpha} \tag{5}$$

where U is the velocity vector; P the pressure; $\tau^{\alpha\beta}$ the viscous stress; F^{α} the exogenic force; and α and β the contravariant indexes.

The discretization form of Eq. (3) can be obtained as follows:

$$\frac{\mathrm{d}U_i^{\alpha}}{\mathrm{d}t}=-\sum_{j=1}^{n}m_j\left(\frac{P_i}{\rho_i^2}+\frac{P_j}{\rho_j^2}\right)\frac{\partial W_{ij}}{\partial x_i^{\alpha}}+\sum_{j=1}^{n}m_j\left(\frac{\mu_i\varepsilon_i^{\alpha\beta}}{\rho_i^2}+\frac{\mu_j\varepsilon_j^{\alpha\beta}}{\rho_j^2}\right)\frac{\partial W_{ij}}{\partial x_j^{\alpha}} \tag{6}$$

where μ is the viscosity coefficient of fluid; and $\varepsilon_i^{\alpha\beta}$ and $\varepsilon_j^{\alpha\beta}$ the strain tensor of particles i and j.

The energy conservation equation is expressed as follows:

$$\frac{\mathrm{d}E}{\mathrm{d}t}=-\frac{p}{\rho}\frac{\partial v^{\beta}}{\partial x^{\beta}}+\frac{\mu}{2\rho}\varepsilon_i^{\alpha\beta}\varepsilon_j^{\alpha\beta} \tag{7}$$

where E is the internal energy.

The discretization form of Eq. (5) can be obtained as follows:

$$\frac{\mathrm{d}E_i}{\mathrm{d}t}=\frac{1}{2}\sum_{j=1}^{n}m_j\left(\frac{P_i}{\rho_i^2}+\frac{P_j}{\rho_j^2}\right)v_{ij}^{\beta}\frac{\partial W_{ij}}{\partial x_i^{\alpha}}+\frac{\mu}{2\rho}\varepsilon_i^{\alpha\beta}\varepsilon_j^{\alpha\beta} \tag{8}$$

2.1.2. Coupled SPH with FEM

Since the coupling problem of SPH/FEM is a three-dimensional problem, the discrete analog of Eq. (1) was needed [25]:

$$f(x)=\sum_{I}W(x-x_I)f(x_I)\Delta V_I \tag{9}$$

where ΔV_I the measure of the domain surrounding node I. In this computation, the initial volume of particles was:

$$\Delta V_I=\frac{m_I}{\rho_I} \tag{10}$$

where m_I is the mass of node I; and ρ_I the density of node I.

Then the approximation can be written in a recognized form as in finite element:

$$f(x)=\sum_{I}\phi_I(x)f(x_I) \tag{11}$$

$$\phi_I(x)=W(x-x_I)\Delta V_I \tag{12}$$

The function $\phi_I(x)$ is the shape function of SPH. The SPH element could be regarded as a special element, which was controlled by node (particle) number and mass. The coupling of SPH and FEM was realized using the penalty method to make the force of particles acting on the finite elements. Thus, the node-to-surface contact was applied in the coupling method of SPH/FEM. In the process of SPH/FEM coupling, particles in SPH were defined as the slave node, while finite elements were defined as the master surface.

2.2. Numerical model

Based on the composite rock-breaking experiment of high-pressure CO_2 jet & PDC cutter, a coupled SPH/FEM numerical model is firstly established, as shown in Fig. 2. The rock model was established by the FEM method and the CO_2 jet model was established by the SPH method. To simulate the experimental case, the numerical rectangular block sample of sandstone with dimensions of 100 mm×100 mm square and a height of 10 mm was established. The rock FEM model has an element size of 2 mm. To accurately observe the rock stress of the cutting region, the cutting region was subdivided from the whole rock sample and the element size of the cutting region was re-meshed again by using finer element size at 0.5 mm which is 1/4 times of the original rock element size. As shown in Fig. 2, the diameter of the CO_2 jet is D_j, the jet impacts the rock surface at a certain angle (ϕ), and the impacting point which is the center point of the impacting region on the rock surface is made in Fig. 2. The distance from the impact point to the PDC cutter is the impact distance (d). The jet would move along the cutting direction with the PDC cutter together at a constant cutting speed (V_c) while impacting obliquely with the rock surface at a certain angle (ϕ). The rake angle (θ) of PDC cutter is 20° (Fig. 3).

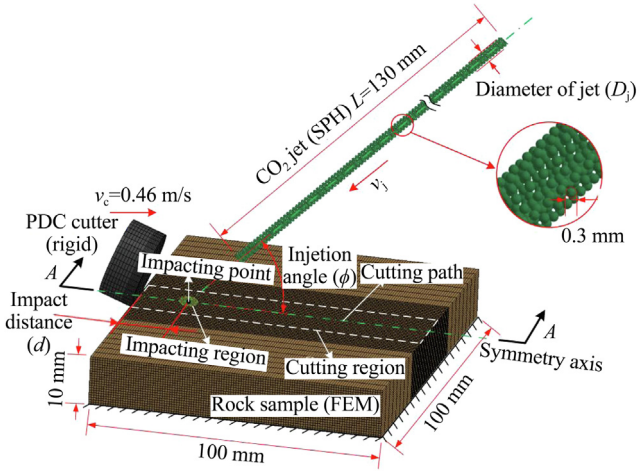

Fig. 2. Geometric model of composite rock-breaking of high-pressure CO_2 jet & PDC cutter.

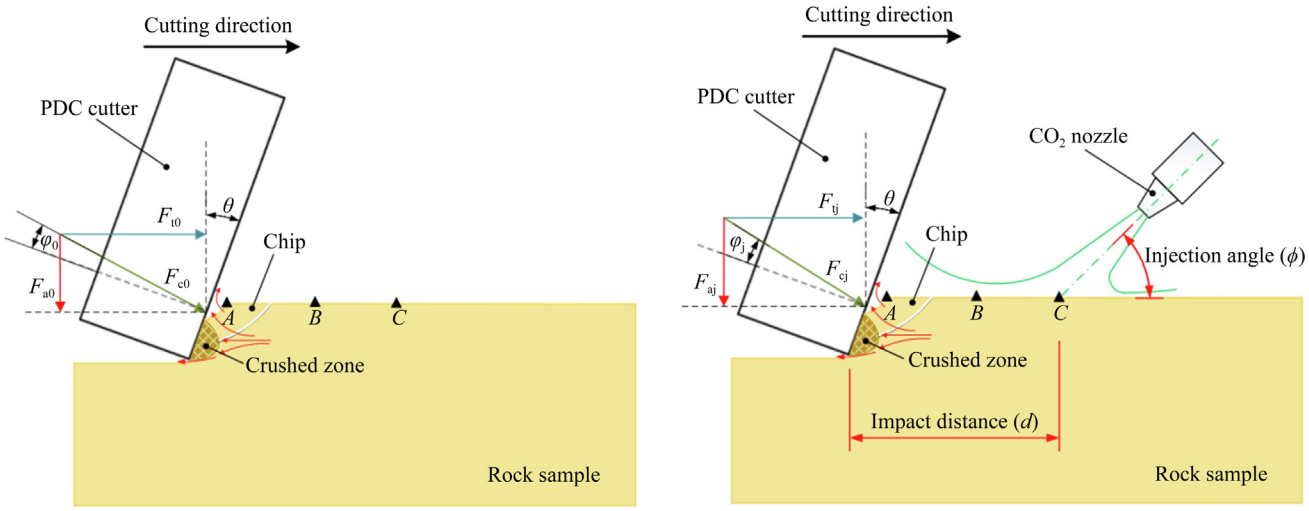

Fig. 3. Mechanical model of single cutter cutting and composite rock-breaking.
Note: F_{c0} is the cutting force without jet; F_{t0} the tangential force without jet; F_{a0} the axial force without jet; F_{cj} the cutting force with jet; F_{tj} the tangential force with jet; F_{aj} the axial force with jet; φ_0 the interface friction angle without jet; and φ_j the interface friction angle with jet.

The interface friction angle (φ) characterizes the frictional interaction between the cutter's rake face and the rock [28].

The problem of mesh deformation can be effectively avoided by using the SPH method, therefore, the flow field and expansion of high-pressure CO_2 jet can be effectively simulated. In the SPH model, the NULL material model and the Mie-Grueisen equation of state are used to define the high-pressure CO_2 jet particles. Based on the variation of CO_2 fluid [29], the material parameters of the high-pressure CO_2 jet are set as shown in Table 1.

The material properties were gained through experiments, as shown in Table 2. The Holmquist-Johnson-Concrete (HJC) material model is applied to the rock model, which can accurately simulate the damage and fracture generation in the rock model. The two common failure modes, tensile stress failure and compressive stress failure, are fully considered in rock cutting simulation. The rock element is simulated by the FEM algorithm, and relatively accurate damage characteristics can be obtained. The material properties of the sandstone constitutive model are shown in Table 3. Three failure criteria in the HJC model are utilized: tensile stress failure, tensile strain failure and shear strain threshold failure.

Eroding-nodes-to-surface is defined as a contact mode for the CO_2 jet (SPH) and rock (FEM). The SPH particles are used as the slave, and the rock elements are used as the master. At the same time, the PDC cutter is defined as a rigid model. Eroding-surface-to-surface is used as a surface contact mode between the PDC cutter and rock element [16]. According to the experimental model, the bottom boundary of the rock is fully constrained (completely fixed). Apart from the cutting surface (upper surface of the rock), other surfaces are defined as transmission boundary conditions. The comparison between experimental and numerical results in composite rock-breaking is shown in Fig. 4.

3. Results and discussion

Based on the results of numerical simulation, the stress field of rock, the cutting force of PDC cutter and the flow field of CO_2 jet composite rock-breaking by high-pressure CO_2 jet & PDC cutter are studied. The effects of CO_2 jet parameters on composites rock breaking were further studied and discussed, such as jet impact velocity, nozzle diameter, jet injection angle and impact distance. Finally, the optimal nozzle arrangement and working parameters are obtained through the researches to improve the rock-breaking efficiency of composite rock-breaking.

3.1. Stress field of rock

The stress field in the rock and the composite rock-breaking process are shown in Fig. 5 (ΔT represents the time interval between the graphs under the same experimental conditions). Before analysis, three points on the top rock surface are selected, which are respectively point *A*, point *B* and point *C*. Point *A* is the rock element in front of the PDC cutter, point *C* the impacting point, and point *B* the midpoint between points *A* and *C*. By extracting the effective stress of points *A*, *B*, and *C*, respectively, it can be found that the effective stress of the point *C* under composite rock-breaking is larger than that under single PDC cutter cutting. But the effective stress of point *B* under composite rock-breaking is lower than that under single PDC cutter cutting. The main reason is that two stress waves in opposite directions are superimposed in this region. At the same time, the cutting action of the PDC cutter is discontinuous. The PDC cutter first cuts into the rock and forms several small chips by crushing the rock until these small chips accumulate and become large enough to form another major chip [18]. Under the condition without jet, the stress concentration

Table 1
Material properties of the high-pressure CO_2 jet state equation.

Parameters	P (MPa)	T_C (K)	ρ_j (g/mm^3)	C_s (m/s)	S_1	S_2	S_3	γ_0
Value	5–40	300	0.879×10^{-3}	1480	2.56	−1.986	0.2286	0.4934

Note: P is the pressure of CO_2 jet; T_C the temperature of high-pressure CO_2; C_s the speed of sound in CO_2; and S_1 S_2 S_3 and γ_0 the constants in the equation of state.

Table 2
Material properties of sandstone sample.

Types of rocks	Density (g/mm^3)	Compressive strength (MPa)	Tensile strength (MPa)	Poisson's ratio
Sandstone	2.26×10^{-3}	77.24	4.56	0.20

Table 3
Parameters of HJC material model.

ρ_0 (g/mm^3)	f_c (MPa)	T (MPa)	G (MPa)	A_1	B_1	C_1	N	S_{max}	D_1	D_2
2.26×10^{-3}	22.79	1.95	1.189×10^4	0.32	1.76	0.0127	0.79	5	0.013	1
EF_{min}	K_1 (MPa)	K_2 (MPa)	K_3 (MPa)	P_{crush} (MPa)	μ_{crush}	P_{lock} (MPa)	μ_{lock}	$\varepsilon_0(s^{-1})$	FS	
0.01	8.1×10^4	9.1×10^4	8.9×10^4	25.3	0.00167	800	0.00167	1	0.5	

Note: ρ_0 is the density of rock; f_c the quasi-static uniaxial compressive strength; T the maximum tensile hydrostatic pressure; G the shear modulus; A_1 the normalized cohesive strength; B_1 the normalized pressure hardening; C_1 the strain rate coefficient; N the pressure hardening exponent; S_{max} the normalized maximum strength; D_1 and D_2 the damage constants; EF_{min} the amount of plastic strain before fracture; K_1 K_2 and K_3 the pressure constants; P_{crush} the crushing pressure; μ_{crush} the crushing volumetric strain; P_{lock} the locking pressure; μ_{lock} the locking volumetric strain; ε_0 the reference strain rate; and FS the failure type.

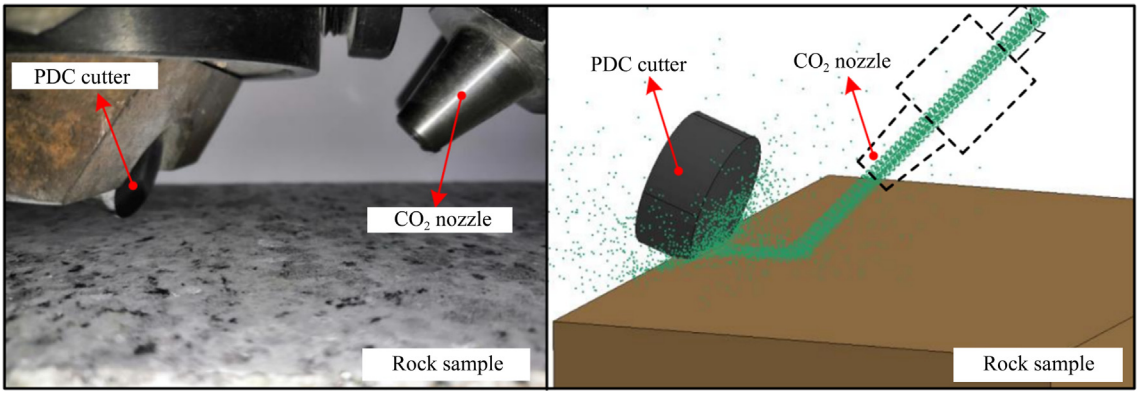

Fig. 4. Comparison between experiment and simulation results in composite rock-breaking.

region on the rock begins at the root of the PDC cutter and forms a crushed zone [19]. With the further cutting of the PDC cutter, the stress concentration region extends from the crushed zone to the rock surface. When the stress value increases to the tensile limit of the rock, the rock chip is peeled off from the main body (Fig. 3). Both under composite rock-breaking and single PDC cutter cutting, the effective stress of point A in the figure is 0 MPa, the main reason is that this point is located on the chip and does not directly contact the PDC cutter.

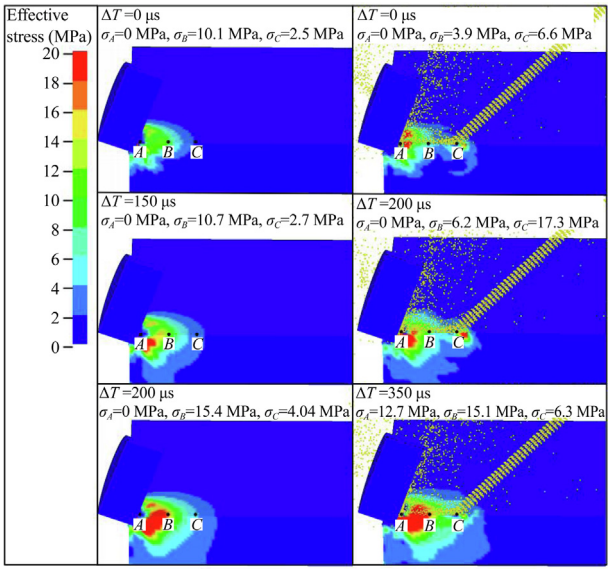

Fig. 5. Comparative analysis of rock stress field during single PDC cutter cutting and composite rock-breaking.

When the jet impacts rock, the stress wave effect induced by the jet impacting is the dominant factor for the fracture generation [30]. It can be found from the study that when the CO_2 jet impacts the top rock surface at the speed of 150 m/s, the rock at impact point C cannot observe obvious fragmentation. The main reason is the diffusion and expansion of the high-pressure CO_2 jet, which makes the high-pressure CO_2 jet non-continuously ejecting from the nozzle and finally reduces the impact load on the top rock surface. Under the jet impingement, the quasi-static pressure of the jet plays a major role in rock breaking [31]. There are two failure criteria in the rock by high-pressure jet impact, respectively, named as shear failure and tensile failure. The shear failure is mainly concentrated below the jet impacting point. Tensile failure mainly occurs in the area far from the jet impacting point, and it dominates the initiation and propagation of radioactive cracks and layered cracks [32]. Damage of the micropores and the microfractures have been found in rock in the later period of rock breaking. Since CO_2 is more likely to invade into micropores and microfractures, large tensile stress forms around the rock crushing pit after volume expansion and pressure relief. This process is the

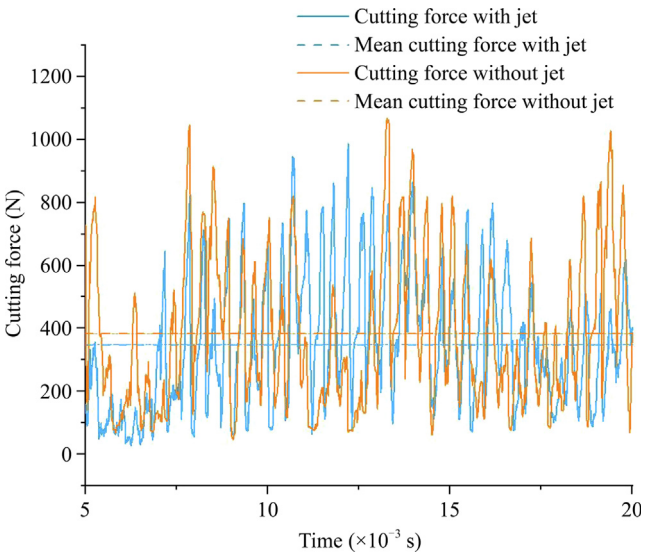

Fig. 6. Dynamic analysis of cutting force on PDC cutter.

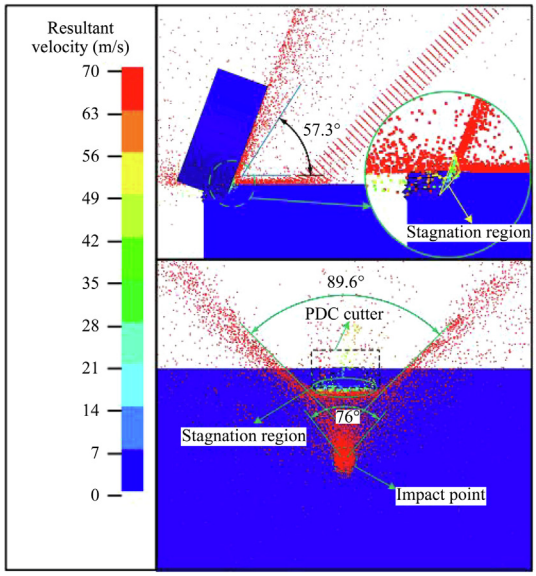

Fig. 7. Analysis of particle velocity of CO_2 jet in the process of composite rock-breaking.

main reason for the threshold pressure reduction of jet rock breaking and the improvement of the rock breaking efficiency [14].

3.2. Cutting force of PDC cutter

Comparing the cutting force (F_c) of the PDC cutter between single PDC cutter cutting and high-pressure CO_2 jet & PDC cutter collaborative cutting by numerical simulation, the dynamic analysis diagram of the cutting force on the PDC cutter is drawn as shown in Fig. 6. During the PDC cutter cutting, the fluctuation of cutting force is the characteristic symbol to reflect the variation of cutting load and rock failure [33]. In addition, the cutting force, an important indicator of the rock cutting processes, is capable of revealing the intrinsic mechanisms of rock breaking quantitatively [34]. By calculating the mean cutting force of single cutter cutting, it can be found that the mean cutting force is 383 N. The variance of the cutting force is 57199 N^2. Under the combined action of the high-pressure CO_2 jet & PDC cutter, the mean cutting force on the PDC cutter reduces to 348 N, and the variance of the cutting force is 42661 N^2. The cutting force of composite rock-breaking reduces by 9.1% compared with single cutter cutting. And the cutting force variance of composite rock-breaking correspondingly reduces by 25.4%. It can be found that the vibration amplitude of cutting force under composite rock-breaking is lower than that under single cutter cutting. When the vibration amplitude is large, it means that the dynamic load on the cutter is also giant, easily resulting in dynamical damage for the PDC cutter. At the same time, the larger the dynamic load, the more significant volume of rock fragments is created. The cutting force of composite rock-breaking fluctuated more frequently and is smaller than that of single PDC cutter cutting. These results indicate that the rock is more easily broken during the composite rock-breaking process, and the volume of debris will be smaller, which can prevent the PDC cutter from being impacted by a great dynamical load. The results show that in the process of composite rock-breaking, the mean cutting force, the peak cutting force and vibration amplitude of the PDC cutter are significantly reduced, which can effectively relieve the influence of vibration and shock on the PDC cutter, and greatly prolong the service life of the PDC cutter.

3.3. Flow field of CO_2 jet

The CO_2 jet particle flow characteristics during the composite rock-breaking process are shown in Fig. 7. It can be seen that when the high-pressure CO_2 jet impacts the top rock surface at an inclination angle of 45°, the jet particles spread radially around. The particles with approximately constant speed move toward the PDC cutter surface in a fan pattern at the angle of 76°. After the jet impacts the surface of the PDC cutter, the flow is divided into two parts: the first part flow to the sides of the PDC cutter, taking away the most cutting debris; the second part flow to the top of the PDC cutter, generating a back-flow. So that the debris generated during the rock breaking process can be quickly and timely carried away from the PDC cutter. In this way, there will be no accumulation of large amounts of debris in front of the PDC cutter. This is why the peak cutting force of the PDC cutter reduces significantly compared with single cutter cutting in Section 3.2. Meanwhile, the velocity of the jet particles at the position between the PDC cutter and the rock decreases significantly, forming a stagnation region. The jet enters this stagnation region under the action of pressure, which can effectively reduce the temperature rising of the PDC cutter.

By comparing the high-speed photography images and the thermal infrared photography of composite rock-breaking and PDC cutter cutting (Fig. 8), it can be found that the rock debris constantly splashes and accumulate in front of the PDC cutter during single cutter cutting. In the process of composite rock-breaking, the jet impacts the rock surface and continues to clean the PDC cutter. After the debris is separated from the rock block, they are quickly carried away from the stagnation region at the front of the PDC cutter. It can decrease the accumulation of chips in front of the PDC cutter, and avoid the energy loss caused by secondary crushing. In Fig. 8, the maximum center temperature of the PDC cutter has decreased from 26 to 12 °C. The jet can effectively reduce the maximum center temperature of the PDC cutter, and prevent the frictional heat generating between the PDC cutter and the rock fragments. Finally, a CO_2 jet can both effectively decrease the thermal wear of the PDC cutter and prolong its service life of the PDC cutter [35]. In conclusion, the high-pressure CO_2 jet has a positive effect on carrying rock debris during the composite

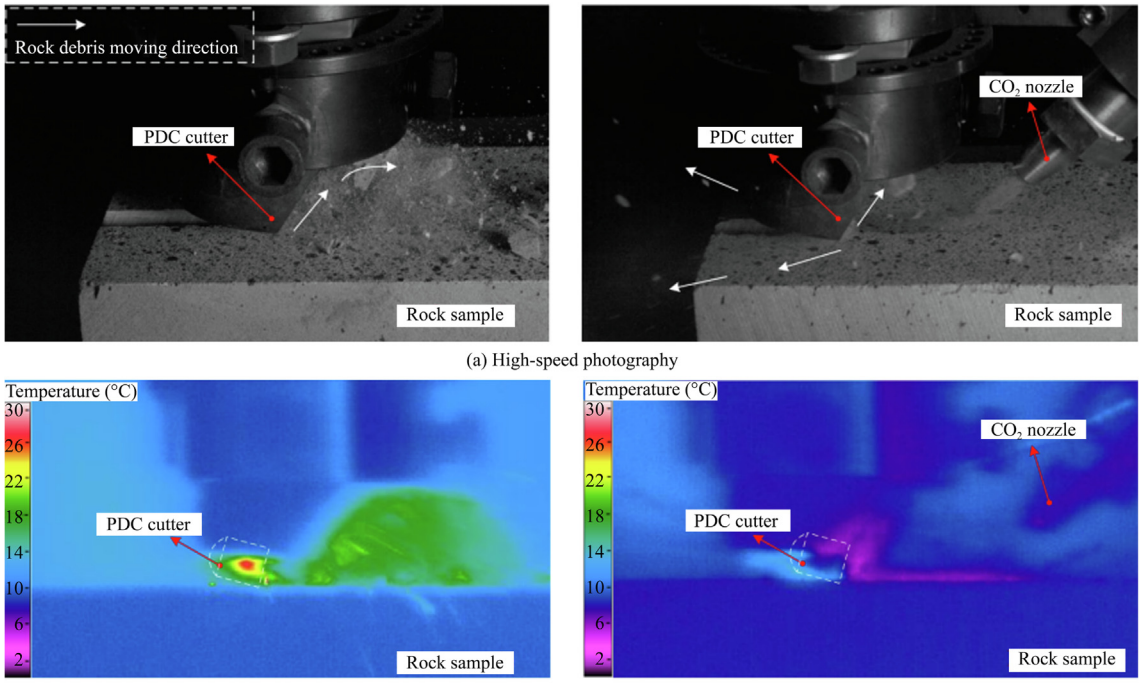

Fig. 8. Results of high-speed photography and thermal infrared photography in the experiment of composite rock-breaking.

rock-breaking, which can effectively reduce the temperature rising and the thermal wear of the PDC cutter.

3.4. Influence of CO_2 jet parameters

In order to analyze the influence of different CO_2 jet parameters on the composite rock-breaking, the numerical simulation of rock breaking without CO_2 jet was carried out first. When the cutting velocity is 0.46 m/s constantly, the cutting depth is 2 mm, the mean cutting force of the PDC cutter is 383 N and the interface friction angle (φ) is 0.9°, the effects of jet parameters, such as impact velocity, nozzle diameter, jet injection angle and impact distance, on the cutting force were discussed respectively.

3.4.1. Impact velocity of CO_2 jet

The variation of mean cutting force (F_m) and interface friction angle (φ) under the different jet velocity are shown in Fig. 9. It can be seen that the values of F_m and φ change slightly when the impact velocity is between 50 and 250 m/s. This is because under the impact of jet, the rock is still in the elastic deformation stage, and even there is a plastic deformation stage and the microfracture initiation, it has not completed failure [12]. However, when the impact velocity of the CO_2 jet is greater than 250 m/s, the mean cutting force decreases significantly. And the contribution of a high-pressure CO_2 jet for composite rock-breaking is obvious. When the CO_2 jet impacts the rock surface, a large number of microfractures is created under the impacting surface, and finally propagates to break the rock into blocks after 1000 μs. Finally, a crushing pit is formed on the rock surface.

It can be seen from the simulation results that the interface force of the jet (F_i) and the effective stress of point C (σ_c) increase with the increase in the impact velocity. As the larger the impact velocity of the CO_2 jet, the greater the kinetic energy load on the rock surface. The stress wave generated by the jet impacting is continuously transmitted along the direction of the PDC cutter and superimposed with the stress wave generated by the PDC cutter. Eventually, both the effective stress of the rock and the influence range of the stress wave increase. Therefore, in the process of composite rock-breaking, the rock is more likely to reach the failure strength, and the cutting force of the PDC cutter would reduce obviously. Interface friction angle (φ) characterizes the frictional interaction between the cutter's rake face and the rock (Fig. 5). The larger the φ is, the more likely the chips would stick to the rake face of the PDC cutter. However, the φ under impact of the CO_2 jet is larger than that without the CO_2 jet, and it increases with the increase in the impact velocity. The reason is that after the jet impacts the rock surface, a layer of pressure water film is formed, which attaches to the rock surface and prevents the tensile failure of rock chips [36].

3.4.2. Nozzle diameter

When the impact velocity of the CO_2 jet is 150 m/s, it can be seen from Fig. 10 that with the increase in nozzle diameter (D_j), the values of mean cutting force, both F_i and σ_c decrease correspondingly. It shows that with the increase in the jet diameter, more energy of the jet load on the rock surface, leading to greater superimposed stress in the rock at the front of the PDC cutter. This made the rock easy to be broken and reduced the cutting force of the PDC cutter. Therefore, it is concluded that increasing the nozzle diameter could reduce the cutting force. When the nozzle diameter is 1 mm, the decrease of cutting force is not obvious. The main reason is that the high-pressure CO_2 jet has high diffusivity and expansion [17], which rapidly reduces the impacting kinetic energy on the rock surface. However, with the increase in nozzle diameter (D_j), the interface friction angle (φ) increases. The main reason is that with the increase in energy, the pressure of the wall jet attached to the rock surface also increases, which hinders the shear failure of rock chips (i. e., the F_a is relatively increased). Therefore, the larger nozzle diameter would provide more severe damage to the rock, but it also results in serious energy loss for the jet. It is found that the optimum range of nozzle diameter is 1.5–2.5 mm.

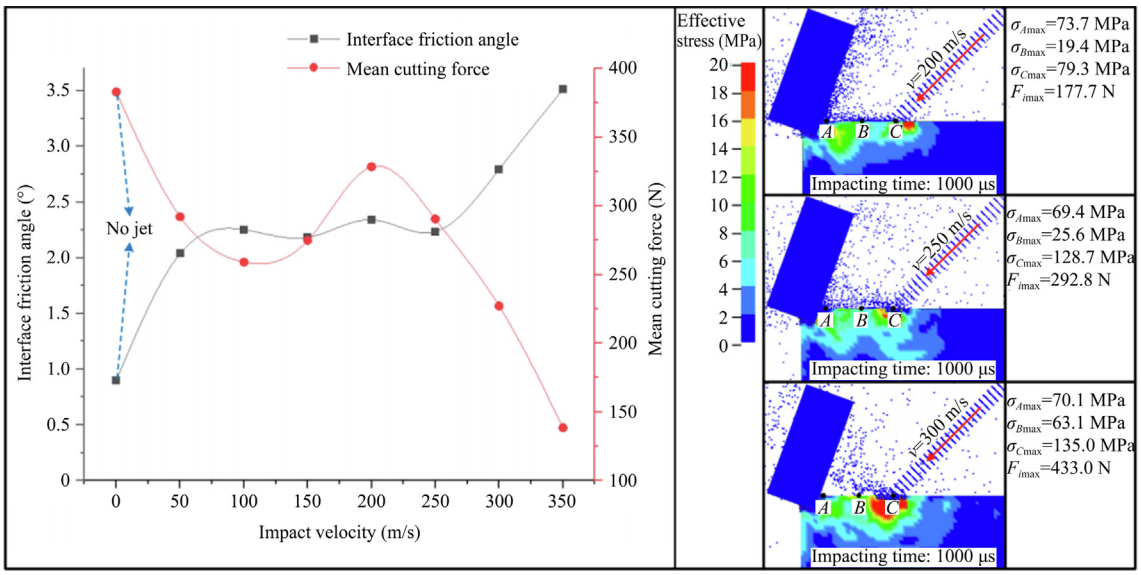

Fig. 9. Variation of mean cutting force and interface friction angle under different impact velocity (No jet when the impact velocity of CO_2 jet is 0 m/s) (V_c=0.46 m/s, θ=20°, D_j=2 mm, ϕ=45°, d=10 mm).

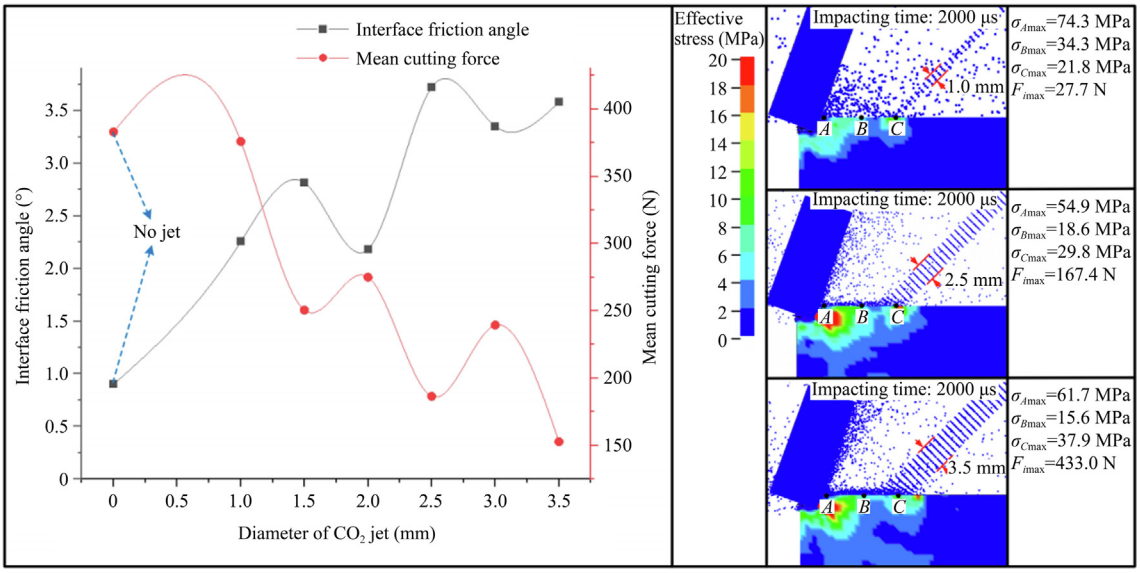

Fig. 10. Variation of mean cutting force and interface friction angle under different nozzle diameter (No jet when the diameter of CO_2 jet is 0 mm) (V_c=0.46 m/s, θ=20°, V_j=150 m/s, ϕ=45°, d=10 mm).

3.4.3. Injection angle of CO_2 jet

The variation of the mean cutting force and the interface friction angle under different injection angles is shown in Fig. 11. It can be seen that in the process of composite rock-breaking, the mean cutting force is greatly reduced compared with that without assisting jet. Especially, when the injection angle of the CO_2 jet is 60°, the mean cutting force is the smallest compared with other injection angles. At this time, the effective stress of the rock at the impact point is larger than other injection angles, and an obvious shear zone is also formed at the impact region. This is because when the injection angle is large, the impact energy of the jet can effectively destroy the rock. When the injection angle is less than 60°, the impact energy of the jet cannot be fully transferred to the rock surface. Therefore, the effective stress at the impact point is smaller than that at the other large injection angle. It can be concluded that the jet with a smaller injection angle has a weaker effect on rock damage [32]. However, when the injection angle is greater than 60°, the mean cutting force increases stably, which is mainly due to the rapid expansion and dispersion of the CO_2 jet after impacting the rock surface. Only a small part of the jet fluid flows to the PDC cutter, which decreases the possibility of rock tensile failure in front of the PDC cutter and reduces the capacity of debris-carrying.

With the increase in the injection angle, the interface friction angle also increases. We observed that the increasing interface friction angle is attributed to the increase in thickness of the wall jet which would prevent the rock chips generation and removing from rock block. In summary, in the process of composite rock-breaking by high-pressure CO_2 jet & PDC cutter, the optimal injection angle of CO_2 jet is 60° [37], the cutting force at this time is the smallest, and the effect of carrying rock debris is the best.

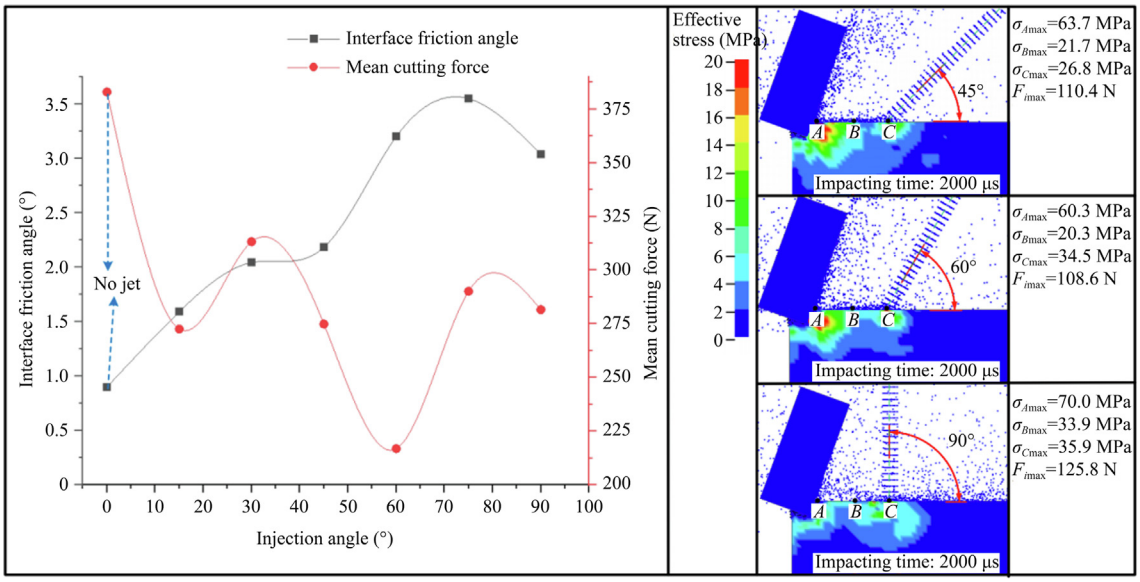

Fig. 11. Variation of mean cutting force and interface friction angle under different injection angle (No jet when the injection angle of CO_2 jet is 0°) (V_c=0.46 m/s, θ=20°, V_j=150 m/s, D_j = 2 mm, d=10 mm).

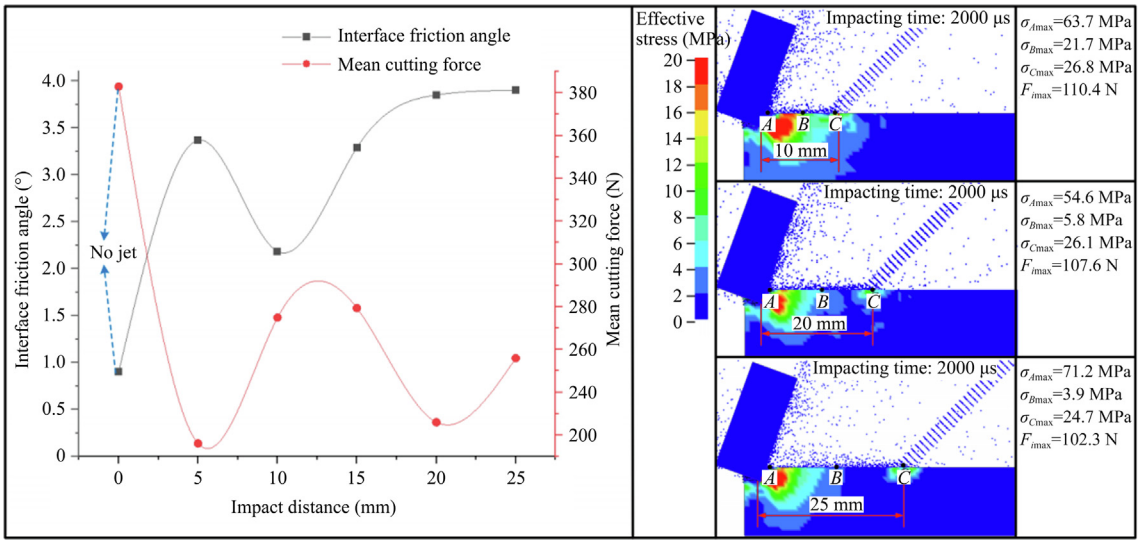

Fig. 12. Variation of mean cutting force and interface friction angle under different impact distance (No jet when the impact distance of CO_2 jet is 0 mm) (V_c=0.46 m/s, θ=20°, V_j=150 m/s, D_j = 2 mm, ϕ=45°).

3.4.4. Impact distance of CO_2 jet

When the impact distance of the CO_2 jet is 2.5 and 10 times the nozzle diameter (D_j=2 mm), the mean cutting force is smaller and the interface friction angle is larger than that of other impact distance (Fig. 12). When the impact distance of the CO_2 jet is 5 mm, the cutting force is the smallest. This is because when the impact region is closer to the PDC cutter, the impingement force of the jet can largely increase the maximum stress of the rock on the front of the cutter edge and improve debris-removing on the front of the cutter surface. Moreover, when the impact distance of the CO_2 jet varied from 10 to 15 mm, the mean cutting force increases. The reason is that the jet formed a layer of pressure CO_2 film on the rock surface at this time, which prevented the rock from breaking away. In this case, the mechanical cutter cannot perform to its full potential [36]. Although the jet at a distance of 2.5 times of the nozzle diameter can offer great support for the composite rock-breaking, this distance is too small to be applied in the rock bit design. This would make the placement of the nozzle very difficult and the nozzle also would block the upward movement of the rock debris. Therefore, considering the nozzle shape and arrangement space, the optimal impact distance is 10 times of the nozzle diameter.

4. Conclusions

Combining experiments and numerical simulations, this paper adopts the coupled SPH/FEM method to study the mechanism of composite rock-breaking from the perspective of rock stress field, cutting force and jet flow field. And the effects of CO_2 jet parameters on composite rock-breaking were further studied and discussed, such as jet impact velocity, nozzle diameter, injection angle and impact distance. The main conclusions are presented as follows:

(1) In the process of composite rock-breaking, CO_2 is more likely to invade into micropores and microfractures, and large tensile stress forms around the rock crushing pit after volume expansion and pressure relief. This process can reduce the threshold pressure of jet rock breaking and improve the rock breaking efficiency. Under the action of the CO_2 jet, the stress value of the rock is more likely to reach its tensile limit, resulting in the chips being peeled off from the main body more easily.

(2) The results show that the cutting force of composite rock-breaking reduces by 9.1% compared with single cutter cutting. And the cutting force variance of composite rock-breaking correspondingly reduces by 25.4%. These results fully prove that in the process of composite rock-breaking, the mean cutting force and vibration amplitude of the PDC cutter have a significant reduction, which can effectively relieve the influence of vibration and shock on the PDC cutter, and greatly prolong the service life of the PDC cutter.

(3) By comparing the high-speed photography images and the thermal infrared photography of composite rock-breaking and PDC cutter cutting, it can be found that the maximum center temperature of the PDC cutter has decreased from 26 to 12 °C. The main reason is that the high-pressure CO_2 jet has a positive effect on carrying rock debris during the composite rock-breaking. Which can effectively reduce the temperature rising and the thermal wear of the PDC cutter, and prolong the service life of the PDC cutter.

(4) In the process of composite rock-breaking, when the impact velocity of the CO_2 jet is less than 250 m/s, there is a large reduction in the mean cutting force, although the CO_2 jet has not directly broken the rock. The optimal range of nozzle diameter is 1.5–2.5 mm, and the best injection angle of CO_2 jet is 60°. Considering the nozzle shape and arrangement position, the optimal impact distance is 10 times the nozzle diameter. The above studies could provide theoretical support and technical guidance for composite rock-breaking of high-pressure CO_2 jet & PDC cutter, which is useful for the CO_2 underbalance drilling and drill bit design.

Acknowledgments

This work was supported by the National Natural Science Foundation of China (No. 52004236), Sichuan Science and Technology Program (No. 2021JDRC0114), the Starting Project of Southwest Petroleum University (No. 2019QHZ009), the China Postdoctoral Science Foundation (No. 2020M673285), the Open Project Program of Key Laboratory of Groundwater Resources and Environment (Jilin University), Ministry of Education (No. 202005009KF), and the Chinese Scholarship Council (CSC) funding (No. 202008515107).

References

[1] Wang HG, Huang HC, Bi WX, Ji GD, Zhou B, Zhuo LB. Deep and ultra-deep oil and gas well drilling technologies: Progress and prospect. Nat Gas Ind B 2021;41(8):163–77.
[2] Tian S, Li G, Huang Z, Niu J, Xia Q. Investigation and application for multistage hydrajet-fracturing with coiled tubing. Petrol Sci Technol 2009;27(13):1494–502.
[3] Xie KC, Li WY, Zhao W. Coal chemical industry and its sustainable development in China. Energy 2010;35(11):4349–55.
[4] Zhu YQ, Romain C, Williams CK. Sustainable polymers from renewable resources. Nature 2016;540(7633):354–62.
[5] Middleton R, Viswanathan H, Currier R, Gupta R. CO_2 as a fracturing fluid: Potential for commercial-scale shale gas production and CO_2 sequestration. Energy Proc 2014;63:7780–4.
[6] Cai C, Kang Y, Wang XC, Hu Y, Chen H, Yuan XH, Yang C. Mechanism of supercritical carbon dioxide (SC-CO_2) hydro-jet fracturing. J CO_2 Util 2018;26:575–87.
[7] Cai C, Kang Y, Yang YX, Liao FL, Chen YF, Huang M, Chen H. Experimental investigation on flow field and induced strain response during SC-CO_2 jet fracturing. J Petrol Sci Eng 2020;195:107795.
[8] Cai C, Li BR, Zhang YY, He W, Yang YX, Kang Y, Wu JW. Fracture propagation and induced strain response during supercritical CO_2 jet fracturing. Petroleum Sci; 2022. Article in press.
[9] Wang M, Huang K, Xie WD, Dai XG. Current research into the use of supercritical CO_2 technology in shale gas exploitation. Int J Min Sci Technol 2019;29(5):739–44.
[10] Li J, Liu GH, Guo BY. Pilot test shows promising technology for gas drilling. J Petroleum Technol 2012;64(7):32–7.
[11] Kolle JJ. Coiled-tubing drilling with supercritical carbon dioxide. Presented at the SPE/CIM International Conference on Horizontal Well Technology, 2000.
[12] He ZG, Li GS, Tian SC, Wang HZ, Shen ZH, Li JB. SEM analysis on rock failure mechanism by supercritical CO_2 jet impingement. J Petroleum Sci Eng 2016;146:111–20.
[13] Cansell F, Aymonier C, Loppinet-Serani A. Review on materials science and supercritical fluids. Curr Opin Solid State Mater Sci 2003;7(4–5):331–40.
[14] Du YK, Wang RH, Ni HJ, Huo HJ, Huang ZY, Yue WM, Zhao HX, Zhao B. Rock-breaking experiment with supercritical carbon dioxide jet. J China Univ Petroleum Ed Nat Sci 2012;36(4):93–6. in Chinese.
[15] Yang SJ, Li J, Liu GH. Influence of low temperature induced by Joule-Thomson effect on rock breaking during gas drilling. J China Univ Petroleum Ed Nat Sci 2016;40(4):90–5. in Chinese.
[16] Jiang Y, Kan T, Pu X, Feng T, Dai Z. Numerical simulation analysis of high-pressure water jet breaking coal parameters based on coupling algorithm of smoothed particle hydrodynamics and finite element method. Saf Coal Mines 2017;48(1):137–40.
[17] Du YK, Wang RH, Ni HJ, Li MK, Song WQ, Song HF. Determination of rock-breaking performance of high-pressure supercritical carbon dioxide jet. J Hydrodyn Ser B 2012;24(4):554–60.
[18] Maurer WC. The state of rock mechanics knowledge in drilling. U.S. Symposium on Rock Mechanics (USRMS), Minneapolis; 1966.
[19] Che DM, Zhu WL, Ehmann KF. Chipping and crushing mechanisms in orthogonal rock cutting. Int J Mech Sci 2016;119:224–36.
[20] He LP, Liu YB, Shen K, Yang XL, Ba QB, Xiong W. Numerical research on the dynamic rock-breaking process of impact drilling with multi-nozzle water jets. J Petrol Sci Eng 2021;207:109145.
[21] Yang C, Hu JH, Ma SW. Numerical investigation of rock breaking mechanism with supercritical carbon dioxide jet by SPH-FEM approach. IEEE Access 2019;7:55485–95.
[22] Lin XD, Lu YY, Tang JR, Ao X, Zhang L. Numerical simulation of abrasive water jet breaking rock with SPH-FEM coupling algorithm. J Vib Shock 2014;33(18):170–6. in Chinese.
[23] Cai C, Gao C, Wang H, Pu Z, Tan Z, Yang X. Flow field and cuttings carrying enhancement mechanism of compound rock breaking by high pressure CO_2 jet and PDC cutters. Nat Gas Ind 2021;41(10):101–8. in Chinese.
[24] Cai C, Yang XP, Gao C, Pu ZC, Zhang P, Tan ZB, Li BR, Xie S. Intense cooling during composite rock breaking of high-pressure CO_2 jet-polycrystalline diamond cutter. SPE J 2022;24:1–16.
[25] Ma L, Bao RH, Guo YM. Waterjet penetration simulation by hybrid code of SPH and FEA. Int J Impact Eng 2008;35(9):1035–42.
[26] Attaway SW, Heinstein MW, Swegle JW. Coupling of smooth particle hydrodynamics with the finite element method. Nucl Eng Des 1994;150(2–3):199–205.
[27] Bian L. The SPH method and its application in hyper velocity impact. Doctoral dissertation. Hefei: University of Science and Technology of China; 2009.
[28] Rostamsowlat I, Richard T, Evans B. An experimental study of the effect of back rake angle in rock cutting. Int J Rock Mech Min Sci 2018;107:224–32.
[29] Cai C, Wang XC, Mao SH, Kang Y, Lu YY, Han XD, Liu WC. Heat transfer characteristics and prediction model of supercritical carbon dioxide (SC-CO_2) in a vertical tube. Energies 2017;10(11):1870.
[30] Huang F, Lu YY, Tang JR, Ao X, Jia YZ. Research on erosion of shale impacted by supercritical carbon dioxide jet. Chin J Rock Mech Eng 2015;34(4):787–94. in Chinese.
[31] Wang RH, Ni HJ. Research of rock fragmentation mechanism with high-pressure water jet. J Univ Petroleum China 2002;26(4):118–22. in Chinese.
[32] Jiang HX, Du CL, Liu SY, Gao KD. Numerical analysis on damage field of rock fragmentation with water jet. J Central South Univ Sci Technol 2015;46(1):287–94. in Chinese.
[33] Dai XW, Huang ZW, Shi HZ, Cheng Z, Xiong C, Wu XG, Zhang HY. Rock failure analysis based on the cutting force in the single PDC cutter tests. J Petroleum Sci Eng 2020;194:107339.
[34] Che DM, Zhang WZ, Ehmann K. Chip formation and force responses in linear rock cutting: An experimental study. J Manuf Sci Eng 2016;139(1):011011.
[35] Hood M, Knight GC, Thimons ED. A review of jet assisted rock cutting. J Eng Ind 1992;114(2):196–206.
[36] Liu XH, Liu SY, Li L, Cui XX. Experiment on conical pick cutting rock material assisted with front and rear water jet. Adv Mater Sci Eng 2015;2015:506579.
[37] Chen JF. Research on configuration method and rock breaking performance of pick assisted with high pressure water jet. Xuzhou: China University of Mining and Technology; 2014.